View metadata, citation and similar papers at core.ac.uk
brought to you by CORE
provided by Elsevier - Publisher Connector

Current Biology, Vol. 13, 598–602, April 1, 2003, ©2003 Elsevier Science Ltd. All rights reserved. DOI 10.1016/S0960-9822(03)00174-X

γ-Tubulin Functions in the Nucleation of a Discrete Subset of Microtubules in the Eukaryotic Flagellum

Paul G. McKean,[1] Andrea Baines,[2,3] Sue Vaughan,[2,3] and Keith Gull[2,3,*]
[1]Department of Biological Sciences
Lancaster University
Lancaster
Lancashire LA1 4YQ
[2]School of Biological Sciences
University of Manchester
2.205 Stopford Building
Oxford Road
Manchester M13 9PT
United Kingdom

Summary

γ-tubulin is an essential part of a multiprotein complex that nucleates the minus end of microtubules. Although the function of γ-tubulin in nucleating cytoplasmic and mitotic microtubules from organizing centers such as the centrosome and spindle pole body is well documented [1–3], its role in microtubule nucleation in the eukaryotic flagellum is unclear. Here, we have used *Trypanosoma brucei* to investigate possible functions of γ-tubulin in the formation of the 9 + 2 flagellum axoneme. *T. brucei* possesses a single flagellum and forms a new flagellum during each cell cycle. We have used an inducible RNA interference (RNAi) approach to ablate expression of γ-tubulin, and, after induction, we observe that the new flagellum is still formed but is paralyzed, while the old flagellum is unaffected. Electron microscopy reveals that the paralyzed flagellum lacks central pair microtubules but that the outer doublet microtubules are formed correctly. These differences in microtubule nucleation mechanisms during flagellum growth provide insights into spatial and temporal regulation of γ-tubulin-dependent processes within cells and explanations for the organization and evolution of axonemal structures such as the 9 + 0 axonemes of sensory cells and primary cilia.

Results and Discussion

As in most eukaryotic cells, the motile flagellum of *T. brucei* possesses a 9 + 2 axonemal structure consisting of 9 outer doublet microtubules and a pair of central singlet microtubules. After the axoneme has exited from the trypanosome, a large macromolecular complex (the paraflagellar rod) extends alongside the axoneme within the flagellum [4]. The 9 + 2 microtubule axoneme is subtended by a canonical 9-triplet microtubule basal body (consisting of A, B, and C tubules) that extends during flagellum formation through a transition zone of 9 doublet microtubules with no central pair (Figures 1A and 1B). A probasal body lies alongside the basal body in G1 of the cell cycle, but, at the G1/S boundary, the probasal body extends and nucleates the formation of a new flagellum (Figure 1C). Coincident with this event is the formation of two new probasal bodies associated with each basal body. As the new flagellum extends, basal bodies separate (so segregating the mitochondrial genome), and mitosis and then cytokinesis occur [5, 6].

Trypanosomes contain a single γ-tubulin gene per haploid genome, and the gene product has been localized to diverse sites within the cell, including the basal body and mitotic spindle poles [7]. To study the function of γ-tubulin in flagellum morphogenesis, we constructed an inducible RNAi vector [8] encoding a fragment of the *T. brucei* γ-tubulin coding sequence and transfected this construct into *T. brucei*. Cells in which the vector had correctly integrated into the genome were selected by using phleomycin and the clonal lines generated. All results shown are from a representative clone. Prior to induction of RNAi, trypanosomes were normal, as judged by morphology, growth kinetics, and motility.

Little difference in growth was seen for the first 48 hr after γ-tubulin RNAi was induced, but thereafter growth was much reduced in comparison to controls (Figure 2A). Characteristic phenotypes were noted over time, and the later phenotypes (observed from 72–96 hr onward) were clearly explicable in terms of those expected from the well-reported role of γ-tubulin in mitotic spindle formation [9–11]. Trypanosomes at these late stages accumulated large nuclei, indicative of a failure of the intranuclear spindle. However, here we focus specifically on an early phenotype (observed from 48 hr postinduction), namely, the appearance of a high number of immotile cells within a morphologically normal population (see Movies 1 and 2 in the Supplemental Data available with this article online for a comparison of a noninduced and an γ-tubulin RNAi-induced cell).

Important for our studies, the trypanosome cell has a useful attribute. It possesses one flagellum and constructs a new flagellum during the cell cycle. Thus, observation of a trypanosome late in the cell cycle reveals one old (the anterior) and one new (the posterior) flagellum (see Figure 1C and Movie 3 in the Supplemental Data). However, observing such cells at 48 hr after γ-tubulin RNAi induction clearly showed that, while the old flagellum displayed normal motility, the new flagellum had no intrinsic motility (see Movie 4 in the Supplemental Data). It is clear that when this cell progresses through cytokinesis, the result would be one motile and one paralyzed daughter trypanosome. Figure 2B shows that over time the number of immotile cells increases such that by 96 hr over 50% of the cells are paralyzed.

To confirm the effectiveness of γ-tubulin RNAi, we monitored levels of γ-tubulin protein at various time points after the addition of tetracycline. Owing to sequence diversity in particular motifs, antibodies to vertebrate and yeast γ-tubulins cannot be used to detect *T. brucei* γ-tubulin. We thus produced a monoclonal antibody that recognizes recombinant *T. brucei* γ-tubulin

*Correspondence: keith.gull@path.ox.ac.uk
[3]Present address: Sir William Dunn School of Pathology, University of Oxford, South Parks Road, Oxford OX1 3RE, United Kingdom.

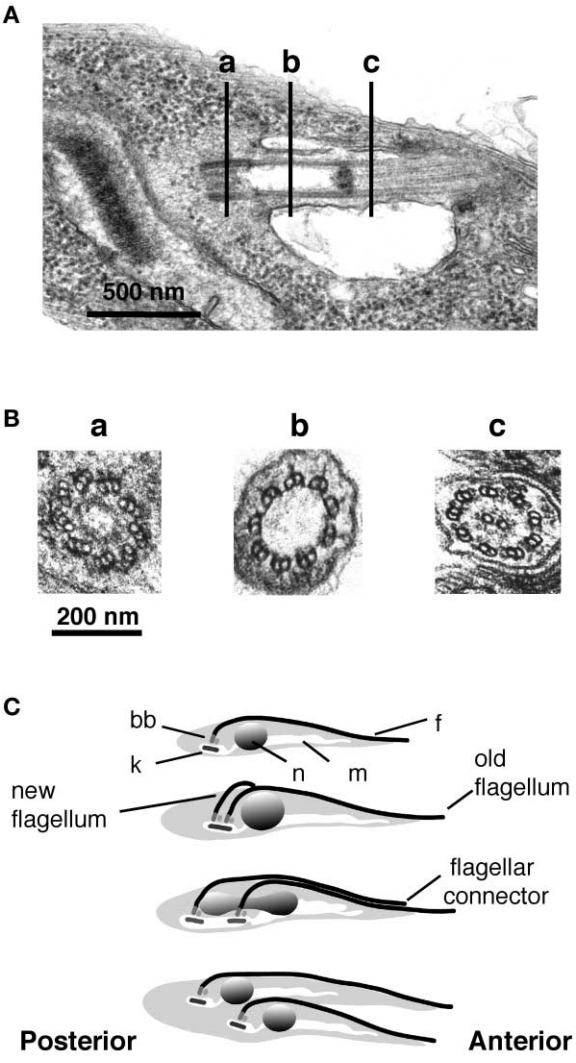

Figure 1. Trypanosomes Construct a Typical Eukaryotic Flagellum Based upon a 9 + 2 Microtubule Axoneme

(A) A thin-section transmission electron micrograph of a longitudinal section through a procyclic *T. brucei* cell showing the flagellum and basal body.

(B) Representative electron micrographs of transverse sections through the basal body and flagellum at positions a, b, and c indicated on Figure 1A.

(C) A schematic showing progressive stages of flagellar morphogenesis during the cell cycle of a procyclic *T. brucei*. n, nucleus; k, kinetoplast; bb, basal body and probasal body; m, mitochondria; f, flagellum. Note that the new flagellum is always positioned posterior to the old flagellum. For an image of a real trypanosome cell in division, see Figure S1 in the Supplemental Data.

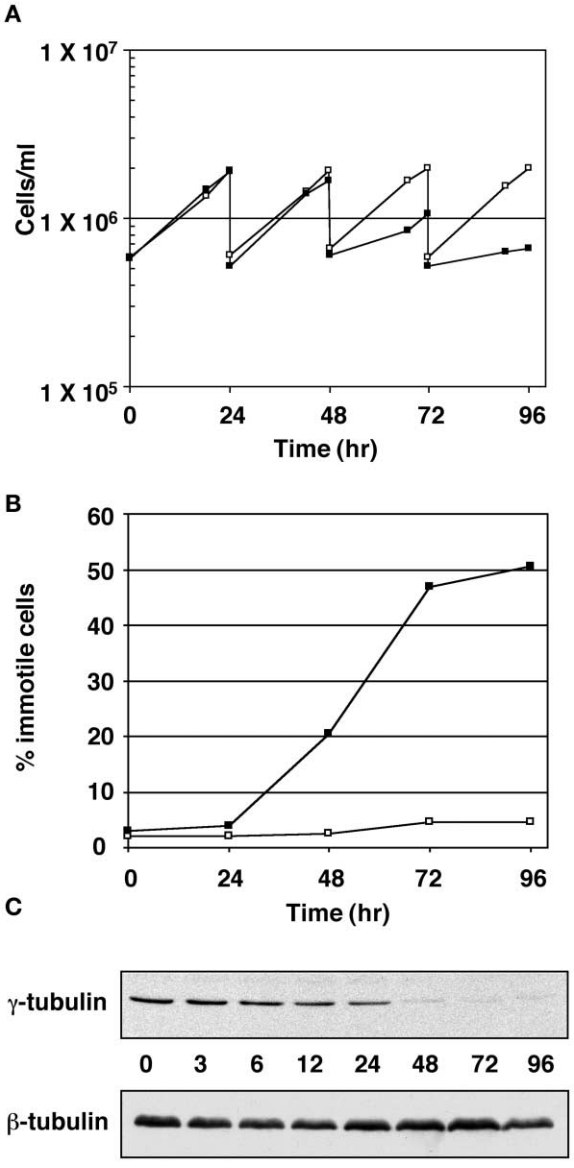

Figure 2. Induction of γ-Tubulin RNAi in *T. brucei* Results in γ-Tubulin Depletion, Growth Arrest, and Cell Paralysis

(A) A graph showing the effect of γ-tubulin RNAi induction upon trypanosome growth (closed squares) compared to a γ-tubulin RNAi-noninduced control (open squares).

(B) A graph showing the generation of paralysis in *T. brucei* cultures following induction of γ-tubulin RNAi (closed squares) compared to a γ-tubulin RNAi-noninduced control (closed squares).

(C) Immunoblots of *T. brucei* total cell lysates collected at various time points after induction of γ-tubulin RNAi probed with monoclonal antibodies raised against γ-tubulin (top panel) and β-tubulin (bottom panel) showing specific depletion of γ-tubulin protein from the γ-tubulin RNAi-induced cells.

and used this to probe immunoblots of trypanosome lysates after RNAi induction. These experiments confirmed that cellular levels of γ-tubulin protein were progressively depleted so that by 48 hr postinduction γ-tubulin protein is barely detectable. In contrast, β-tubulin levels (β-tubulin acts as both a loading and specificity control in these experiments) remain unaffected during the time course of the experiment (Figure 2C). Unfortunately, this anti-γ-tubulin antibody is ineffective in immunolocalization studies.

To understand the paralysis of the new flagellum, we fixed and processed γ-tubulin RNAi-induced trypanosomes for analysis by thin-section electron microscopy. Given the early phenotype of a paralyzed new flagellum and a motile old flagellum, we searched specifically for cells late in their cell cycles with two flagella (Figure 3). One can know with certainty which is the old and which

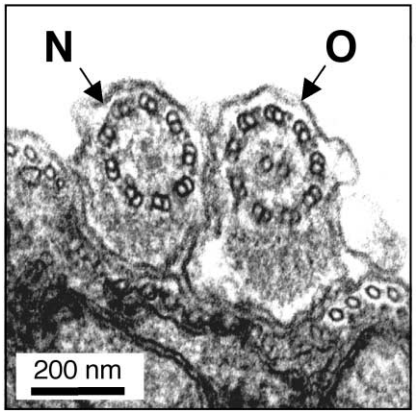

Figure 3. γ-Tubulin Depletion Results in the Construction of a 9 + 0 Microtubule Axoneme in the New Flagellum

A thin-section transmission electron micrograph of a procyclic *T. brucei* cell showing that a canonical 9 + 2 microtubule axoneme has been constructed in the old flagellum (O) but that an atypical 9 + 0 microtubule axoneme is present within the new flagellum (N).

	9+2	9+0	9+1
	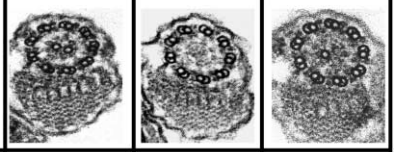		
γ -tubulin RNAi Noninduced	100%	0%	0%
γ -tubulin RNAi Induced	45%	44.2%	8.9%

Figure 4. Quantification of the Effect of γ-Tubulin Depletion on Flagella Central Pair and Outer Doublet Microtubule Nucleation

A total of 260 axonemes from γ-tubulin RNAi-noninduced and γ-tubulin RNAi-induced procyclic cells were analyzed by transmission electron microscopy and categorized based upon the presence/absence of central pair and outer doublet microtubules. Representative transmission electron micrographs of the major structural categories observed are shown, along with the frequency at which each type was present expressed as a percentage of the total number of axonemes observed.

is the new flagellum in *T. brucei* because the new flagellum is always present on the left-hand side of the old flagellum when the cell is viewed from the posterior end [5]. This polarity can be determined in electron micrographs because of the axial polarity of the outer microtubule doublets and associated dynein arms. Examination of the cell in Figure 3 reveals a dramatic difference between the old and new flagellum. The new flagellum, constructed under conditions of depleted γ-tubulin, lacks both of the central pair microtubules but has a normal complement of 9 outer doublet microtubules. Although the presence of central pair microtubules is not absolutely required for axonemal motility (for instance, nodal cilia in mammals have a 9 + 0 axoneme but are able to beat and are important in establishing left-right asymmetry in developing embryos [12]), it is clear that the axonemes of most motile cilia/flagella do exhibit a 9 + 2 arrangement of microtubules. The role of the central pair appears to lie in providing an enhanced degree of control over cilia/flagella beating, and there has been strong evolutionary pressure to conserve the 9 + 2 structure.

We quantified this differential effect on central pair and outer doublet flagellum microtubules by analyzing 260 cross-sections of flagella from both control (noninduced) and experimental (γ-tubulin RNAi-induced) 72 hr populations (Figure 4). Control axonemes showed a 9 + 2 microtubule configuration. However, under γ-tubulin RNAi-induced conditions, only 45% of axonemes exhibited the canonical 9 + 2 configuration; 44.2% exhibited a 9 + 0 microtubule configuration, 8.9% exhibited a 9 + 1 configuration, and a few (1.9%) exhibited a n + 0 configuration, in which one or more outer doublets were also absent. In the case of the 9 + 1 axonemes, we have no evidence to suggest a differential effect on either the C1 or C2 central pair microtubule. These studies provide direct evidence that γ-tubulin functions to nucleate the central pair microtubules during flagellum morphogenesis but that nucleation of the outer doublet microtubules is a γ-tubulin-independent phenomenon involving extension from pre-existing triplet microtubules of the basal bodies/centrioles. Thus, these results add a third cellular compartment to the existing two (nucleus and cytoplasm) in which γ-tubulin appears to be absolutely required for de novo nucleation of microtubules. Importantly, the involvement of γ-tubulin in diverse microtubule organizing centers (MTOCs) in any one cell may explain why γ-tubulin-dependent nucleation events such as centriole/basal body duplication and flagellum central pair nucleation are often observed to occur at G1/S in a variety of protists and metazoan cells. This would have the effect of temporally separating regulation of these events from those involved in the critical nucleation of the mitotic spindle.

There also appears to be a role for γ-tubulin in the earlier nucleation of the triplet microtubules of the centriole/basal body. Ruiz and colleagues, studying basal body duplication in *Paramecium*, have shown that γ-tubulin has just such a role in this ciliate [13]. Our observations suggest that continued growth under conditions of γ-tubulin depletion (for periods longer than discussed here) also results in the nucleation of aberrant basal bodies (data not shown). Thus, a γ-tubulin-dependent nucleation step appears to be essential to centriole/basal body duplication. The nucleation of aberrant basal bodies (completely lacking triplet microtubules at certain positions within the basal body structure) would also explain the few n + 0 axonemes (axonemes with no central pair and in which the outer doublet number varies from 9) that we observed at the 48 hr time point. There is no doubt that these effects on basal body construction itself will increase with time but become overtaken by the late phenotype of mitotic/cell division arrest due to lack of γ-tubulin nucleation of cytoplasmic and spindle microtubules.

Although it has long been accepted that basal bodies act as the MTOCs for eukaryotic flagella/cilia, the molec-

ular mechanisms leading to axonemal microtubule nucleation are not well understood. Our results show a clear distinction between nucleation of central pair microtubules (a γ-tubulin-dependent process) and outer doublet microtubules (a γ-tubulin-independent process). The latter appears to require only the pre-existing template of the basal body/centriole triplet microtubules. Examination of the known structures within the basal body suggests that the transition zone is key to the explanation. Central pair nucleation occurs from a central structure at the distal end of the transition zone (see Figure 1A). We suggest that this central structure serves to anchor two γ-tubulin complexes capable of nucleating the two central axonemal microtubules. Indeed, Silflow and colleagues have localized γ-tubulin to precisely this location in the basal body transition zone in the green algae *Chlamydomonas* [14], and our previous studies localized *T. brucei* γ-tubulin to the basal body [7].

Specialized cilia are now recognized as providing sensory functions in a range of metazoans, and these cilia usually possess axonemes with a 9 + 0 configuration. The 9 + 0 axoneme is a characteristic feature of the primary cilium formed as an extension of the mature centriole in many cells within the mammalian body and in cells in culture in the G1/G0 phase of the cell cycle [15]. There is recent evidence that the primary cilium exhibits specific receptors, and malfunction of this cilium leads to disease in mammals [16, 17]. The 9 + 0 axoneme is also found in sensory cells of invertebrates such as *C. elegans* and in the modified sensory cilia of vertebrate photoreceptors [18, 19]. The distinction between central pair and outer doublet nucleation that we have described here provides opportunities for differential regulation of microtubule extension into a 9 + 2 or a 9 + 0 axoneme. It appears likely that, during the normal proliferative cell cycle in mammalian cells or certain sensory cell differentiations, the γ-tubulin-containing distal transition zone central structure is not formed on the mature centriole. Thus, the cell forms a 9 + 0 cilium that operates as a specific sensory organelle within the differentiated cell. Finally, defective assembly of axonemal central pair microtubules has also been observed in the motile cilia and sperm of individuals with diseases such as primary cilia dyskinesia (PCD) [20, 21]. Given that central pair nucleation is dependent upon the construction of a γ-tubulin complex within the distal central transition zone, identification of its molecular components may provide candidate genes for some of these primary ciliary dyskinesias.

Experimental Procedures

Trypanosome Growth

Procyclic *T. brucei* strain 29-13 (kindly provided by George Cross, Rockerfeller University, New York), which contains the genes encoding T7 RNA polymerase and tetracycline repressor [22], was grown in SDM-79 media supplemented with 15% fetal calf serum, 15 μg ml^{-1} G418, and 50 μg ml^{-1} hygromycin. Cell growth was monitored by using a CASY1 cell counter and analyzer system (Schärfe System GmbH), and cultures were diluted on a daily basis to maintain a density between 5×10^5 and 5×10^6 cells per milliliter.

Plasmid Construction and Parasite Transfection

A 500 nucleotide fragment of the *T. brucei* γ-tubulin coding sequence was amplified by PCR with *T. brucei* γ-tubulin-specific primers γRNAiF (5′-CTCGAGCAAATATACAGTCTTCTGTGC-3′) and γRNAiR (5′-AAGCTTTCAAAAGTTTCGTATATAATC-3′) and was cloned into the TA cloning vector pGEMT-Easy (Promega). Following confirmation of the correct (wild-type) nucleotide sequence, the γ-tubulin DNA fragment was excised by using HindIII and XhoI restriction sites (underlined) and was cloned into the inducible RNAi vector pZJM [8]. Trypanosomes were transfected by using standard protocols [23], were selected by using 2.5 μg ml^{-1} phleomycin, 15 μg ml^{-1} G418, and 50 μg ml^{-1} hygromycin, and were subsequently cloned by limiting dilution.

Induction of RNA Interference and Analysis of Motility

Trypanosome cultures were placed in drug-free media for 24 hr prior to the initiation of RNAi studies and were then diluted to 5×10^5 cells per milliliter, and tetracycline was added to a final concentration of 1 μg ml^{-1}. Cultures were counted and diluted back to a density of 5×10^5 cells per millilieter every 24 hr, and fresh tetracycline was added to the culture medium. For analysis of motility, trypanosomes were placed on a haemocytometer slide and were viewed on an inverted stage microscope at 20× magnification with a Nikon TMS microscope. For each time point, 200 cells were closely observed, and cells were scored on the basis of the presence or absence of motility. Video sequences were made on a Leica DMRBE microscope equipped with differential interference contrast optics with a COHU high-performance charge coupled device camera, and images were processed by using Scion Image 1.62a software (NIH, USA) as previously described [24].

Expression and Purification of Recombinant γ-Tubulin

Recombinant γ-tubulin was expressed and purified as described previously [7] and then further purified by preparative SDS-PAGE and electroelution.

Generation of Monoclonal Antibodies

BALB/c mice were immunized with purified recombinant γ-tubulin and hybridomas produced as described previously [25].

Protein Sample Preparation and Western Blotting

Trypanosomes (2×10^8) were collected at various time points after the addition of tetracycline and were washed once in phosphate-buffered saline containing a cocktail of protease inhibitors. Cells were boiled in Laemmli sample buffer, separated by 10% SDS-PAGE, and electroblotted onto a nitrocellulose membrane (2×10^6 cells per lane). Membranes were probed for 2 hr at room temperature with primary antibodies at the following dilutions: anti-γ-tubulin monoclonal antibody was used neat; the β-tubulin-specific monoclonal antibody KMX [26] was used at a dilution of 1:500. Membranes were then probed with HRP-conjugated anti-mouse secondary antibodies for 1 hr. Blots were developed by using an ECL detection system (Amersham).

Electron Microscopy

Trypanosomes were prepared for transmission electron microscopy as described previously [5], except for the omission of tannic acid during the fixation procedure.

Supplemental Data

Supplemental Data including four movies that illustrate both the normal motility of the trypanosome flagellum as well as the paralyzed flagellar phenotype that results following γ-tubulin RNAi induction are available at http://images.cellpress.com/supmat/supmatin.htm. An annotated image of a trypanosome undergoing cytokinesis is also presented, enabling a direct comparison to be made between these movies and the schematic representation of flagellar morphogenesis shown in Figure 1C.

Acknowledgments

We thank Hui Lu for assistance with electron microscopy and members of the Gull lab for helpful comments and discussions. This work was supported by a Programme Grant from The Wellcome Trust.

Received: October 17, 2002
Revised: January 8, 2003
Accepted: February 11, 2003
Published: April 1, 2003

References

1. Jeng, R., and Stearns, T. (1999). Gamma-tubulin complexes: size does matter. Trends Cell Biol. *9*, 339–342.
2. Schiebel, E. (2000). γ-tubulin complexes: binding to the centrosome, regulation and microtubule nucleation. Curr. Opin. Cell Biol. *12*, 113–118.
3. Wiese, C., and Zheng, Y. (1999). γ-tubulin complexes and their interaction with microtubule-organising centers. Curr. Opin. Struct. Biol. *9*, 250–259.
4. Gull, K. (1999). The cytoskeleton of trypanosomatid parasites. Annu. Rev. Microbiol. *53*, 629–655.
5. Sherwin, T., and Gull, K. (1989). The cell cycle division of *Trypanosoma brucei brucei*: timing of event markers and cytoskeletal modulations. Philos. Trans. R. Soc. Lond. B. Biol. Sci. *323*, 573–588.
6. Robinson, D.R., and Gull, K. (1991). Basal body movements as a mechanism for mitochondrial genome segregation in the trypanosome cell cycle. Nature *352*, 731–733.
7. Scott, V., Sherwin, T., and Gull, K. (1997). γ-tubulin in trypanosomes: molecular characterisation and localisation to multiple and diverse organising centres. J. Cell Sci. *110*, 157–168.
8. Wang, Z., Morris, J.C., Drew, M.E., and Englund, P.T. (2000). Inhibition of *Trypanosoma brucei* gene expression by RNA interference using an integratable vector with opposing T7 promoters. J. Biol. Chem. *275*, 40174–40179.
9. Lajoie-Mazenc, I., Detraves, C., Rotaru, V., Gares, M., Tollon, Y., Jean, C., Julian, M., Wright, M., and Raynaud-Messina, B. (1994). Recruitment of antigenic γ-tubulin during mitosis in animal cells: presence of γ-tubulin in the mitotic spindle. J. Cell Sci. *107*, 2825–2837.
10. Spang, A., Geissler, S., Grein, K., and Schiebel, E. (1996). γ-tubulin-like Tub4p of *Saccharomyces cerevisiae* is associated with the spindle pole body substructures that organise microtubules and is required for mitotic spindle formation. J. Cell Biol. *134*, 429–441.
11. Khodjakov, A., and Rieder, C.L. (1999). The sudden recruitment of γ-tubulin to the centrosome at the onset of mitosis and its dynamic exchange throughout the cell cycle, does not require microtubules. J. Cell Biol. *146*, 585–596.
12. Nonaka, S., Tanaka, Y., Okada, Y., Takeda, S., Harada, A., Kanai, Y., Kido, M., and Hirokawa, N. (1998). Randomization of left-right asymmetry due to loss of nodal cilia generating leftward flow of extraembryonic fluid in mice lacking KIF3B motor protein. Cell *95*, 829–837.
13. Ruiz, F., Beisson, J., Rossier, J., and Dupuis-Williams, P. (1999). Basal body duplication in Paramecium requires γ-tubulin. Curr. Biol. *9*, 43–46.
14. Silflow, C.D., Liu, B., LaVoie, M., Richardson, E.A., and Palevitz, B.A. (1999). γ-tubulin in *Chlamydomonas*: characterisation of the gene and localisation of the gene product in cells. Cell Motil. Cytoskeleton *42*, 285–297.
15. Lange, B.M.H., and Gull, K. (1996). Structure and function of the centriole in animal cells: progress and questions. Trends Cell Biol. *6*, 348–352.
16. Hou, X., Mrug, M., Yoder, B.K., Lefkowitz, E.J., Kremmidiotis, G., D'Eustachio, P., Beier, D.R., and Guay-Woodford, L.M. (2002). Cystin, a novel cilia-associated protein, is disrupted in the cpk mouse model of polycycstic kidney disease. J. Clin. Invest. *109*, 533–540.
17. Yoder, B.K., Huo, X., and Guay-Woodford, L.M. (2002). The polycystic kidney disease proteins, polycystin-1, polycystin-2, polaris, and cystin, are co-localised in renal cilia. J. Am. Soc. Nephrol. *13*, 2508–2516.
18. Qin, H., Rosenbaum, J.L., and Barr, M.M. (2001). An autosomal recessive polycystic kidney disease gene homolog is involved in intraflagellar transport in *C. elegans* ciliated sensory neurons. Curr. Biol. *11*, 457–461.
19. Pazour, G.J., Baker, S.A., Deane, J.A., Cole, D.G., Dickert, B.C., Rosenbaum, J.L., Witman, G.B., and Besharse, J.C. (2002). The intraflagellar transport protein, IFT88, is essential for vertebrate photoreceptor assembly and maintenance. J. Cell Biol. *157*, 103–113.
20. Cowan, M.J., Gladwin, M.T., and Shelhamer, J.H. (2001). Disorders of ciliary motility. Am. J. Med. Sci. *321*, 3–10.
21. Tamalet, A., Roudot-Thoraval, F., Desmarquest, P., Roger, G., Boule, M., Millepied, M.C., Baculard, T.A., and Escudier, E. (2001). Abnormal central complex is a marker of severity in the presence of partial ciliary defect. Pediatrics *108*, E86.
22. Wirtz, E., Leal, S., Ochatt, C., and Cross, G. (1999). A tightly regulated inducible expression system for conditional gene knock-outs and dominant-negative genetics in *Trypanosoma brucei*. Mol. Biochem. Parasitol. *99*, 89–101.
23. Bastin, P., Sherwin, T., and Gull, K. (1998). Paraflagellar rod is vital for trypanosome motility. Nature *391*, 548.
24. Moreira-Leite, F.F., Sherwin, T., Kohl, L., and Gull, K. (2001). A trypanosome structure involved in transmitting cytoplasmic information during cell division. Science *294*, 610–612.
25. Woods, A., Sherwin, T., Sasse, R., MacRae, T.H., Baines, A.J., and Gull, K. (1989). Definition of individual components within the cytoskeleton of *Trypanosoma brucei* by a library of monoclonal antibodies. J. Cell Sci. *93*, 491–500.
26. Birkett, C.R., Foster, K.E., Johnson, I., and Gull, K. (1985). Use of monoclonal antibodies to analyse the expression of multi-tubulin family. FEBS Lett. *187*, 211–218.